Coplanar Molecular Assemblies of Amino- and Perfluorinated Alkylsilanes: Characterization and Geometric Definition of Mammalian Cell Adhesion and Growth

David A. Stenger,*,† Jacque H. Georger,‡ Charles S. Dulcey,† James J. Hickman,*,§ Alan S. Rudolph,† Thor B. Nielsen,⊥ Stephen M. McCort,∥ and Jeffrey M. Calvert†

Contribution from the Code 6090, Naval Research Laboratory, Washington, DC 20375, Geo-Centers, Inc., Fort Washington, Maryland 20744, Science Applications International Corporation, McLean, Virginia 22102, Naval Medical Research Institute, Bethesda, Maryland 20889, and National Institute of Alcohol Abuse and Alcoholism, Rockville, Maryland 20852.
Received September 10, 1991. Revised Manuscript Received June 3, 1992

Abstract: The photochemistry of organosilanes was used to (1) create mixed monolayers having continuously adjustable surface free energies and (2) affect high resolution adhesion and spatial orientation of biological cells on silica substrates. Monolayers were formed from two materials, an aminoalkylsilane, $NH_2(CH_2)_2NH(CH_2)_3Si(OCH_3)_3$ (EDA), and a perfluorinated alkylsilane, $CF_3(CF_2)_5(CH_2)_2Si(CH_3)_2Cl$ (13F), and were characterized by ellipsometry and water contact angle measurements. Deep UV (193 nm) radiation was used to induce photochemical changes in the cell-adhesive EDA monolayers. X-ray photoelectron spectroscopy indicated that the amine groups of EDA were removed by the exposure, leaving only Si-OH or alkyl fragments having ≤3 carbons. The exposed substrates were then reacted with 13F to form mixed monolayers or hydrophobic monolayers that inhibited cell adhesion in the irradiated regions. The degree of 13F reactivity with EDA in the unirradiated regions was observed to be solvent-dependent, suggesting that conformational states of the surface amine groups lead to a reduction in their accessibility. The selective photochemistry was exploited to produce high resolution molecular patterns, defined using patterned irradiation, that were mapped with scanning Auger electron spectroscopy. The patterns were used to spatially control the adhesion and direct the outgrowth of rat hippocampal neurons and porcine aortic endothelial cells in vitro. Patterns of controlled geometry may provide new approaches to the study of surface-directed growth, intercellular communication, and organogenesis or be used to control the alignment of individual cells with transducer elements in biosensors and implants.

Introduction

Recent reports have indicated that monolayer systems can be targeted for a variety of applications, including cell adhesion and patterning.[1,2] Several techniques have been introduced in the past few years for the production of patterned self-assembled monolayers (SAMs) of organic functionalities.[2,3] One approach utilizes conventional photoresist methodology to produce high resolution patterns for the adhesion and growth of cells.[2] A fundamentally new technique involves direct modification of SAMs by patterned deep UV exposure.[4,5] Molecules in the exposed regions of a SAM absorb the radiation and undergo photocleavage to yield surface residues. These residues can then be modified with a second type of functionality. This technique offers several distinct advantages over previous methods, most notably a small number of processing steps, sub-half micron resolution (approximately 0.3 μm), and compatibility with a large number of substrate types.[5]

In this paper we report the formation of coplanar molecular patterns consisting of an alkylamine silane, $NH_2(CH_2)_2NH(CH_2)_3Si(OCH_3)_3$ (EDA), and a perfluorinated alkylsilane, $CF_3(CF_2)_5(CH_2)_2Si(CH_3)_2Cl$ (13F). The EDA provides a positively charged, hydrophilic surface that has proven effective in promoting cell adhesion,[2] while the hydrophobic 13F surface has been shown to minimize cell adhesion. We have previously reported preliminary results on the selective adhesion of a neural cancer cell line on patterns prepared from these materials.[4] However, few details were provided on the formation and physical properties of the EDA/13F system. Here, the formation, composition, and physical properties of the pure films and mixed monolayers are characterized by ellipsometry, water contact angle measurements, X-ray photoelectron spectroscopy (XPS), and Auger electron spectroscopy (AES). Also, for the first time, precise geometric control of the adhesion and growth of explanted mammalian neural and endothelial cells is demonstrated using patterns created by deep UV lithography. This is accomplished using patterns designed to promote specific types of cell alignment and interaction.

This study also indicates that it is unnecessary for these monolayers to be well-ordered or oriented to achieve controllable wettability or selective adhesiveness, which encourages the use of a wider variety of silane functionalities. By "tuning" the reactivity at the interface with UV radiation, both mixed monolayers having precisely controlled compositions and high resolution SAM patterns can be geared to a variety of promising studies and applications.

Experimental Section

Chemicals. EDA (*N*-(2-aminoethyl)(3-aminopropyl)trimethoxysilane) and 13F (tridecafluoro-1,1,2,2-tetrahydrooctyl-1-dimethylchlorosilane) were used as received from Hüls of America, Petrarch Silanes. Anhydrous (<0.005% H_2O) methanol and toluene were obtained from Aldrich. Other reagents used were chloroform (Baker; 0.75% ETOH), acetonitrile (Baxter Healthcare), and hexane (Fisher Scientific). All silane reagents were opened, stored, and dispensed under a dry (<1 ppm H_2O) helium atmosphere. All water was deionized to ≥17.6 MΩ/cm resistance. Two model amine compounds, *tert*-butylamine, $(t\text{-Bu})NH_2$, and dibutylamine, $(n\text{-Bu})_2NH$, were obtained from Aldrich.

SAM Formation. The 3" × 1" glass microscope slides (Fisher Scientific), 1" × 1" fused silica slides (Dell Optics), and 50-mm diameter ⟨100⟩ n-type silicon wafer (Recticon) substrates were cleaned by immersion in 1:1 methanol/HCl for at least 30 min at room temperature, rinsing thoroughly in water, and immersion in concentrated H_2SO_4 for at least 30 min. Platinum surfaces were prepared by resistive evaporation

† Naval Research Laboratory.
‡ Geo-Centers, Inc. Current address: Shipley Company, Inc., Marlboro, MA 01752-3092.
§ Science Applications International Corporation.
⊥ Naval Medical Research Institute.
∥ National Institute of Alcohol Abuse and Alcoholism. Current address: U.S. Food and Drug Administration, Rockville, MD 20857.

(1) Swalen, J. D.; Allara, D. L.; Andrade, J. D.; Chandross, E. A.; Garoff, S.; Israelachvili, J.; McCarthy, T. J.; Murray, R.; Pease, R. F.; Rabolt, J. R.; Wynne, K. J.; Yu, H. *Langmuir* **1987**, *3*, 932-950.
(2) Kleinfeld, D.; Kahler, K. H.; Hockberger, P. E. *J. Neurosci.* **1988**, *8*, 4098-4120.
(3) Laibinis, P. E.; Hickman, J. J.; Wrighton, M. S.; Whitesides, G. M. *Science* **1989**, *245*, 845-847.
(4) Dulcey, C. S.; Georger, J. H.; Krauthamer, V.; Stenger, D. A.; Fare, T. L.; Calvert, J. M. *Science* **1991**, *252*, 551-554.
(5) Calvert, J. M.; Dulcey, C. S.; Georger, J. H.; Peckerar, M. C.; Schnur, J. M.; Calabrese, G. S.; Sricharoenchaikit, P. *Solid State Tech.* **1991**, *34*, 77-82.

0002-7863/92/1514-8435$03.00/0

of platinum onto silicon wafers and oxidized using the H_2SO_4 treatment. All cleaned substrates were transferred to boiling water for 15–30 min prior to reaction with silanes. EDA SAMs were formed by immersing cleaned substrates in freshly mixed 94% acidic methanol (1.0 mM acetic acid in methanol), 5.0% H_2O, and 1.0% EDA for 15 min at room temperature and then rinsing three times in methanol. All percentages were in v/v. 13F SAMs were formed by immersing clean or irradiated (vide infra) EDA substrates in a solution of 1.0–2.0% 13F in either toluene, hexane, chloroform, or acetonitrile for 0.5–3 h at room temperature and then rinsing three times with the same solvent. Following the final rinse step in both the EDA and 13F preparations, slides were baked on a hotplate at 120 °C for 5 min. The baking step was performed to quickly remove residual solvent and promote the complete reaction of the silanes. All SAM formation steps were performed in a class 100 clean room or in a Vacuum Atmospheres drybox with a helium atmosphere.

The quality of EDA SAMs was sometimes observed to be dependent on the duration of time between the mixture of EDA with acidic methanol and the addition of water. Delays of more than 20 min led to nonuniform surface coverage and partial polmerization of EDA in solution prior to deposition. These phenomena were evidenced by large variations in the advancing water contact angle measurements across a substrate surface and visible bulk film formation, respectively. In all cases reported here, water was added to the EDA/methanol mixture within 3 min, and the reaction with substrates was initiated immediately afterwards. Conversely, the quality of 13F SAMs was relatively independent of the reagent mixing and reaction times. 13F SAMs exhibited nearly identical properties for reaction times of 30 min and 3 h. The same was true both for 13F films formed on native substrates and on irradiated EDA-treated substrates that were exposed to >10 J/cm^2 (see below).

Contact Angle Measurements. Contact angles were measured by application of static, sessile drops (5–30 μL) of deionized water to the substrate surfaces with a micropipetter. The measurements were made visually on both sides of the drops using a Zisman type goniometer. The advancing contact angle, θ_a, was taken as the maximum contact angle observed as the drop size was incrementally increased without an increase in the contact area. The average values of at least three measurements performed on each modified substrate region were recorded. Measured values of θ_a for a given film were within 3° across the substrate surfaces, indicating macroscopically uniform surface coverages.

Ellipsometry Measurements. Film thickness measurements were made using a Gaertner Model L115C ellipsometer equipped with a helium-neon laser (632.8 nm) light source. The angle of incidence was 70°, and the compensator was set at −45°. All measurements were performed on the polished surfaces of the silicon wafers. These surfaces were determined by ellipsometry to have a native oxide thickness of approximately 20 Å. The optical constants were determined for at least four spots on each individual wafer after cleaning. The wafers were then silanized within 15 min after making the measurements. The thickness of each type of film was calculated using the Gaertner Waferscan software for a single organic thin film. This executes a computational enhancement[6] of the algorithm originally described by McCrackin et al.[7] We made the assumption that the substrate can be represented as a single layer having a set of optical constants that is a combination of the contributions from both silicon and the surface oxide.[8,9] For each film, the thickness was measured at 49 points in an X–Y grid across four different substrates using the predetermined optical constants and a choice of the refractive index, n_f, for each film. In all cases, the precision of the 49 point measurements was reflected by low standard deviation values (~1 Å). However, thicknesses determined in this way have an inherent limitation in accuracy of ±2 Å.[8,9] All thickness values reported in this paper are assumed to be limited to this accuracy.

The estimation of ultrathin organic film thickness by optical ellipsometry is highly dependent on an appropriate choice of the refractive index n_f of the film-forming material. Ellipsometry has been successfully used to measure the thickness of monolayers formed from alkanethiols on gold[10] and long-chain alkyltrichlorosilanes on silica surfaces.[11] Both types of molecules form controllable, ordered structures, lending themselves to the assumption that the monolayers are both uniform and homogeneous. Thus, choices of 1.45–1.50 for n_f (comparable to the refractive index of paraffins) have proven effective for estimating the thickness of these films.[12] In contrast, no known ellipsometric studies have been performed on EDA or 13F thin films. In light of this, we began our investigation by considering the physical plausibility of several choices of n_f for these compounds. The manufacturer-listed[13] refractive index of EDA is 1.442 at 25 °C, while those of representative model compound alkylamine compounds (e.g., ethylenediamine, n_f = 1.46)[14] do not differ greatly. The manufacturer-listed[13] value of n_f for 13F of 1.345 is, however, significantly different from that of perfluorohexane (1.25).[14] We also considered further decreases in the effective value of n_f of these materials, which would be anticipated if the films are highly disordered or loosely packed.

Scheme I. Schematic Model of Patterned EDA/13F SAM Formation[a]

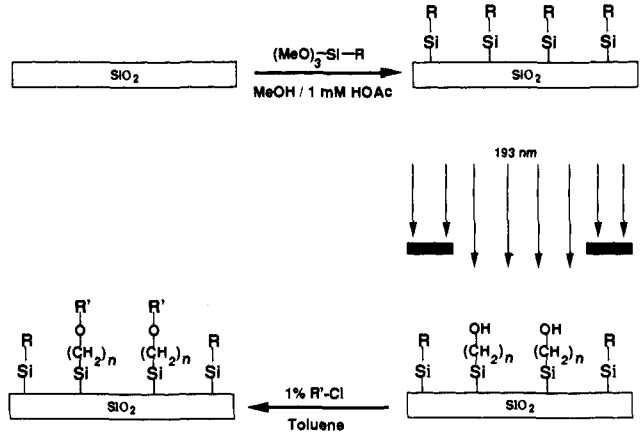

[a] A hydroxyl-rich silica surface (here SiO_2) is reacted with a 1% solution of a trimethoxy alkyl silane, here R = $-(CH_2)_3NH(CH_2)_2NH_2$. The EDA is irradiated with deep UV, causing photolytic removal of most or all of the alkylamine component. Reactive intermediates are generically represented as free hydroxyl groups. This is only for the purpose of indicating renewed reactivity to silanes. 13F reacts in a subsequent step to form coplanar SAMs (R′ = $(CH_3)_2Si(CH_2)_2(CF_2)_5CF_3$).

^{1}H NMR Spectroscopy. Deuterated benzene, C_6D_6 (Cambridge Isotope Labs), was dried over benzophenone/ketyl and degassed prior to use. Samples were prepared under an inert atmosphere using standard Schlenk techniques or in a Vacuum Atmospheres drybox. In each case, an excess (10 μL) of either (*t*-Bu)NH_2 or (*n*-Bu)$_2$NH was added to 10 μL (0.033 mM) of 13F in 0.4 mL of C_6D_6. NMR spectra were obtained using an IBM Bruker AM 250 NMR equipped with a dual ^{1}H/^{13}C probe. Insoluble precipitate was centrifuged to the bottom of the NMR tube prior to data collection.

Deep Ultraviolet Irradiation and Pattern Formation. Individual 3 cm^2 areas of EDA-treated surfaces were exposed to 193-nm deep UV radiation using a Questek Model 2430 ArF excimer laser. Deep UV pulses, having single shot power densities of 100–600 kW/cm^2, were delivered at a 30-Hz repetition rate. Patterned exposures were performed by positioning the EDA-treated surfaces of the substrates tightly against the metalized surface of a fused silica photolithographic mask. A 3" × 3" fused silica mask was used, which had the desired geometrical features defined by a pattern of metal (chrome) on one surface. The metal features on the mask protected regions of the EDA from exposure to the deep UV irradiation. Immediately following the exposures, the substrates were immersed in a 1.0–2.0% (v/v) mixture of 13F *in* toluene, in an attempt to selectively remodify the exposed regions. The overall pattern forming process is shown in Scheme I. Mixed films of EDA and 13F were formed in the same way except that the EDA-treated substrates were exposed to intermediate levels (1–15 J/cm^2) of *unpatterned* 193-nm radiation (no lithographic mask used).

X-ray Photoelectron Spectroscopy (XPS). XPS spectra were obtained on a SSX-100 spectrometer (Surface Science Instruments) equipped with a concentric hemispherical analyzer. The instrument was operated in a fixed analyzer transmission mode using a monochromatic Al Kα X-ray source. The pass energy was 50 eV with a 600 μm spot size. The take-off

(6) Reinberg, A. R. *Applied Optics* **1972**, *11*, 1273–1274.
(7) McCrackin, F. L.; Passaglia, E.; Stromberg, R. R.; Steinberg, H. L. *J. Res. Natl. Bur. Stand. Sect. A* **1963**, *67*, 363–377.
(8) Wasserman, S. R.; Whitesides, G. M.; Tidswell, I. M.; Ocko, B. M.; Pershan, P. S.; Axe, J. D. *J. Am. Chem. Soc.* **1989**, *111*, 5852–5861.
(9) Azzam, R. M. A.; Bashara, N. M. *Ellipsometry and Polarized Light*; North Holland Publishing Company: Amsterdam, 1977.
(10) Chidsey, C. E. D.; Loiacono, D. N. *Langmuir* **1990**, *6*, 682–691.
(11) Wasserman, S. R.; Tao, Y.-T.; Whitesides, G. M. *Langmuir* **1991**, *5*, 1074–1087.
(12) Ulman, A. *Introduction to Ultrathin Organic Films*; Academic Press, Inc.: San Diego, CA, 1991.
(13) *1992 Hüls Silicon Compounds Register and Review*; Hüls America Inc.: Piscataway, NJ.
(14) *CRC Handbook of Chemistry and Physics*, 61st ed.; CRC Press, Inc.: Boca Raton, FL, 1980.

angle was 35°, and the normal operating pressure was approximately 10^{-9} Torr. When nonconducting fused silica substrates were used, the samples were charge neutralized with a 2-5 eV electron beam. In these cases, the electron beam inhomogeneity was eliminated with a fine mesh gold screen. All spectra were referenced to both the C(1s) peak at 284.6 eV and the Si(2p3/2) peak at 102.4 eV of the fused silica. The N(1s) and F(1s) peak areas were normalized to the silicon peak area for each sample.

Auger Electron Spectroscopy (AES). AES was performed on a PHI 660 scanning auger microprobe. The general conditions and precautions necessary for examining monolayers by AES have been previously reported.[15] In our experiments, an 8 kV beam at 4 nA was used for the scanning electron micrograph (SEM) images, Auger element surveys, and single element line scans. Surface charging was minimized by using n-type silicon substrates for all AES experiments.

Cell Culture. Prior to cell plating, the patterned substrates were sterilized by immersion in 70% or pure ethanol for 30 min. Porcine aortic endothelial cells were isolated, established in culture as described,[16] and seeded onto EDA/13F patterns. Hippocampi were removed from fetal rats[17] on the 18th or 19th day of gestation. Cells were dissociated, plated at a density of 10^4–10^6 cells/cm^2, and cultured on inverted glass above an 80% confluent layer of astrocytes as previously described,[18] except that EDA/13F patterns instead of polylysine were used as the growth substrate.

Results

a. Characterization of EDA and 13F SAMs by Wettability and Ellipsometry. The initial value of θ_a of 17–18° (obtained immediately after the bake step) for pure EDA SAMs did not increase with increasing reaction times in the range of 15–60 min. However, these films exhibited time-dependent values of θ_a, which began increasing immediately after baking and reached a steady-state value of 28–32° within 4–5 h. To our knowledge, no reports have been made of EDA film thickness as determined by optical ellipsometry. The choice of $n_f = 1.44$ resulted in an estimated EDA film thickness of 4 ± 2 Å. A hypothetical decrease in the effective value of n_f to as low as 1.35 (which might occur if the film is highly disordered or loosely packed) resulted in an increase in the estimated thicknesses to 5 ± 2 Å. In both cases, the measured thickness was considerably less than that predicted for molecules that are fully extended normal to the substrate surface (~10 Å). However, these results were the same for two different wafers each at EDA reaction times of 15, 30, and 60 min, indicating that the measured thickness values were not attributable to insufficient reaction times.

A θ_a value of 94 ± 2° was obtained for pure 13F films, which was the same regardless of the solvent (chloroform, hexane, toluene, or acetonitrile) used for deposition and did not change significantly for at least several days. Ellipsometric film thickness measurements on 13F films were performed by assuming a range of values for n_f between that of 13F (1.345)[13] or an appropriate model compound, perfluorohexane (1.25).[14] These values resulted in estimated thickness values of 4 ± 2 and 5 ± 2 Å, respectively. Both estimates were significantly less than that predicted for the fully extended molecule (~12 Å). The measured thickness did not change with increasing 13F reaction times (in the range of 2–6 h). This suggested that like EDA, the molecules had formed reaction site- (accessible surface Si–OH) limited monolayers.

b. Photolysis of EDA and Reaction of Residues with 13F. A distinguishing feature of this approach to mixed monolayer formation is that the chemical modification of the first film is accomplished directly and controllably using varying dosages of UV energy. The energy available from 193-nm photons (148 kcal/mol) is more than sufficient to cleave any of the covalent bond types[19] within the SAM. If photolysis of the SAM molecules in air results in the generation of oxidized surface groups (such as –Si–OH or –C–OH), the irradiated surface can react with another organosilane in a subsequent chemical reaction step. An important objective of this study was to investigate this process in further detail.

A first set of experiments was designed to monitor the UV dosage dependence of the photolytic degradation of EDA SAMs on silica substrates and the subsequent reactivity of the irradiated surface with 13F. Individual 3 cm^2 areas were irradiated with a desired UV dosage. Exposure times varied from seconds to as long as 5 min to achieve integrated energy dosages of 1–15 J/cm^2. XPS was used to monitor the surface composition of the irradiated regions following different amounts of exposure. Pure EDA surfaces exhibited N(1s) peaks at 399 and 401 eV (Figure 1, top), characteristic of amine and protonated amine groups, respectively. This result was similar to previously reported observations[20,21] and indicated that some amine groups became protonated by acetic acid during the deposition process. Figure 1 (middle and bottom) also demonstrates the removal of nitrogen and replacement with fluorine following deep UV dosages of 3 and 15 J/cm^2 and retreatment with 13F. SAMs that were exposed to an intermediate radiation energy showed a decrease in the N(1s) peak area, as observed for 3 J/cm^2 (middle). At an energy of 15 J/cm^2, no nitrogen could be detected (bottom). The increasing size of the fluorine peak with increasing radiation dosage was proportional to the decrease of the nitrogen peaks. Ellipsometric measurements were also performed on irradiated areas of EDA-treated silicon wafers at UV dosages that were sufficient to remove the entire N(1s) XPS peak, showing that the decreased thickness of 4–5 Å corresponded to that measured for the intact EDA film.

A second set of experiments was designed to provide evidence on the nature of the photocleavage product(s) and remaining surface residues. First, XPS spectra were obtained from EDA SAMs that were prepared on a platinum oxide substrate and irradiated. In these experiments, the Si(2p) peak of the EDA silicon atom was monitored to see if its area changed after UV exposure. The result was that the silicon peak remained throughout the deep UV exposure range of 0–30 J/cm^2, which resulted in a complete removal of nitrogen. This indicated that a dominant mechanism involves cleavage at the Si–C or a C–C bond. Fourier transform mass spectroscopy experiments were also performed in order to detect the photolysis of EDA SAMs using single pulses of 193-nm radiation.[22] The major peaks were concentrated in the ranges of 92–101 and 82–88 amu, which correspond to the approximate mass of the entire alkylamine component of EDA and the alkylamine component less one $-CH_2-$ group, respectively. These data collectively showed that surface EDA molecules are cleaved at or near the Si–C bond, implying that silanol and/or very short chain alkyl residues (≤3 carbons) form the principal reactive sites for 13F in the irradiated areas.

c. Properties of Mixed Films. We studied the properties of the mixed EDA/13F films, as this was an opportunity to develop a system where the surface wettability could be precisely and reproducibly adjusted. The mixed EDA/13F films were formed by treating EDA-treated fused silica surfaces with 13F in toluene following intermediate UV dosages in the range of 0–15 J/cm^2. Figure 2 (top) plots the changes of the N(1s) and F(1s) XPS peak areas of mixed EDA/13F SAMs against the dose of deep UV received by the initial EDA SAM prior to 13F retreatment in toluene. Significant deviation from a total normalized peak area [N(1s) + F(1s)] of 1.0 may be due to (1) partial contamination of the EDA-treated surfaces with 13F following low UV dosages, (2) incomplete oxidation of the surface, permitting less than monolayer formation by 13F, even after all nitrogens have been

(15) Hickman, J. J.; Ofer, D.; Zou, C.; Wrighton, M. S.; Laibinis, P. E.; Whitesides, G. M. *J. Am. Chem. Soc.* **1991**, *113*, 1128–1132.
(16) Robinson, D. H.; Kang, Y.-H.; Deschner, S. H.; Nielsen, T. B. *In Vitro Cell Dev. Biol.* **1990**, *26*, 169–180.
(17) Banker, G. A.; Cowan, W. M. *Brain Res.* **1977**, *126*, 397–425.
(18) Abele, A. E.; Scholz, K. P.; Scholz, W. K.; Miller, R. J. *Neuron* **1990**, *2*, 413–419.
(19) Walsh, R. *Acc. Chem. Res.* **1981**, *14*, 246.
(20) Moses, P. R.; Wier, L. M.; Lennox, J. C.; Finklea, H. O.; Lenhard, J. R.; Murray, R. W. *Anal. Chem.* **1978**, *50*, 576–585.
(21) Elliot, C. M.; Murray, R. W. *Anal. Chem.* **1976**, *48*, 1247–1254.
(22) EDA samples on native silicon oxide were studied by laser desorption Fourier transform mass spectrometry as previously described (see ref 4) in an attempt to identify primary photoproducts. Upon irradiation at relatively high power at 193 nm (ca. 5 mJ/cm^2/shot) photoproduct ions were observed, corresponding to the EDA parent ion $NH_2(CH)_2(NH)(CH_2)_3$ as well as ions at lower mass. Unlike most other films studied by this technique, at these powers EDA was found to ionize without the use of post-laser ionization by electron beam.

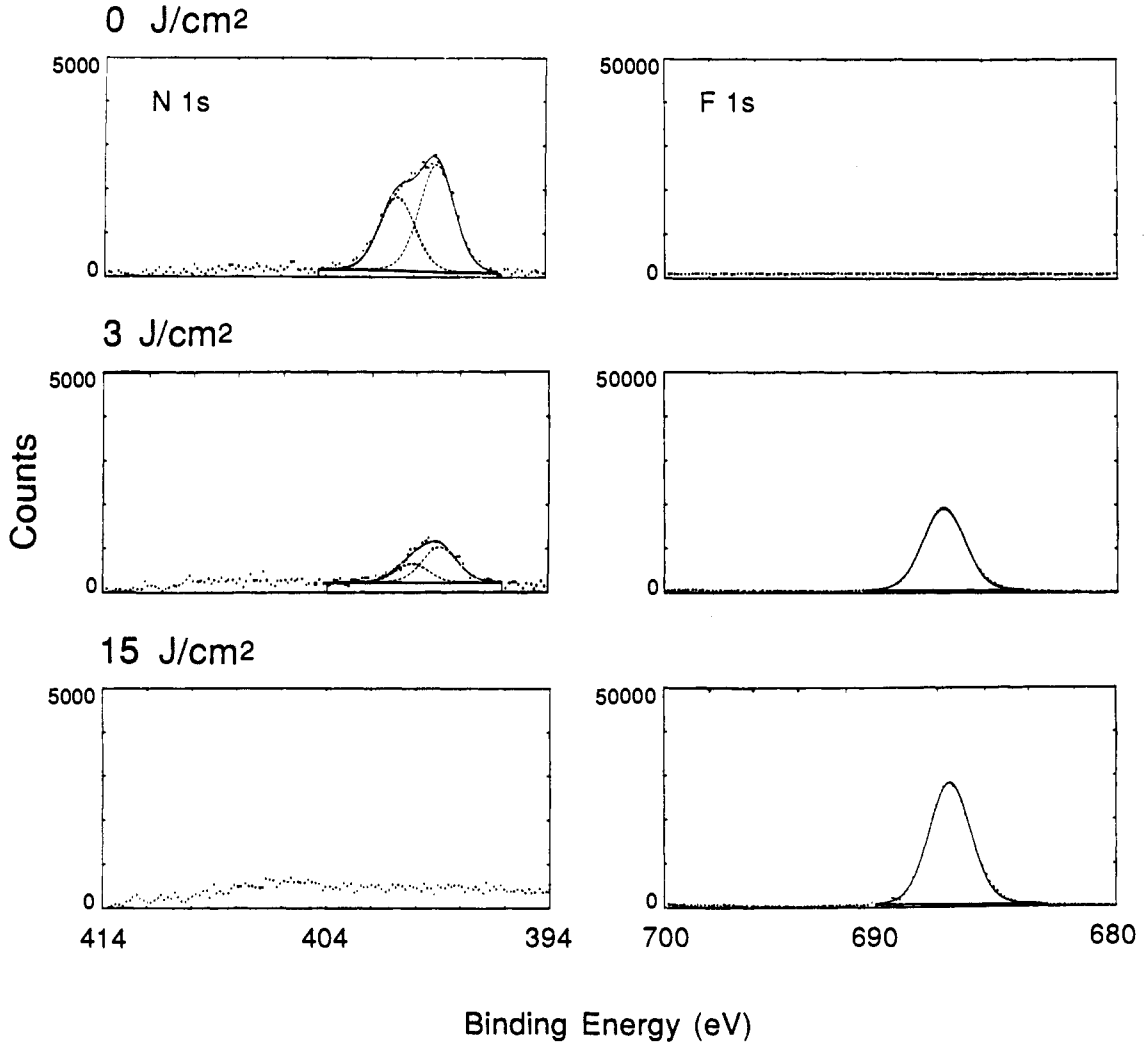

Figure 1. High resolution XPS scans of the N(1s) region (left) and F(1s) region (right) with increasing 193-nm deep UV irradiation. Top: EDA SAM prior to irradiation or treatment with 13F. Note that the two peaks in the N(1s) region correspond to the amine (399 eV) and protonated amine (401 eV) groups in EDA. Middle: EDA SAM after a 3 J/cm^2 deep UV exposure, followed by retreatment with 13F in toluene. Bottom: EDA SAM after a 15 J/cm^2 deep UV exposure, followed by retreatment with 13F in toluene.

removed (such as at 10 J/cm^2), and (3) differences in the packing densities and reaction site accessibility of the two types of molecules. However, the overall rates of decrease of the N(1s) areas were closely paralleled by the rates of increase of the F(1s) areas, indicating a nearly stoichiometric replacement of the photolyzed EDA with 13F.

Previous work by Bain and Whitesides[23,24] has demonstrated the importance of comparing the composition of multiple component alkanethiol monolayers with their wettability. This relationship can be used to infer information concerning the structure of monolayer components and their interactions. The middle plot in Figure 2 shows that the cos θ_a, which is proportional to the surface free energy of the film,[12,25] gradually decreased to that of a pure 13F monolayer at dosages >10 J/cm^2. This confirmed that the original EDA film was completely and functionally replaced with the equivalent of a 13F monolayer formed on cleaned silica surfaces. The relationship between the cos θ_a and the calculated mole fraction of EDA, X_{eda}, is shown in the bottom plot of Figure 2. The cos(θ_a) and X_{eda} exhibited a relationship approaching linearity. The near linearity throughout the entire x-axis depended on the use of the *initial* value of θ_a of 17–18° to calculate the value of cos θ_a at $\chi_{eda} = 1.0$. Interpretation of this relationship using Cassie's law[12,26] would indicate that the two monolayer components interact separately with the wetting solvent.[23,24] Applied to this case, it suggests that the hydrogen bonding of the polar amine groups of EDA with water occurs without significant interference, due to interactions of EDA with itself or with 13F. While this interpretation may be overly simplified,[27] it supports the overall claim that the mixed monolayers are predominantly composed of only *two* species. However, the observed relationship is in contrast with the deviation from linearity observed in mixed films of polar/nonpolar alkanethiols.[23,24]

The bottom plot in Figure 2 includes X_{eda} points at 0.86 and 1.00, that were obtained for unirradiated EDA substrates which were exposed and not exposed to 13F in toluene, respectively. XPS experiments performed on EDA surfaces exposed to 13F in toluene indicated that about one 13F molecule had reacted per six EDA molecules. The subject of the possible 13F reaction site(s) on the EDA-treated surfaces is discussed in detail in the following section. However, it is important to note that even as 13F was incorporated into the EDA films, the nearly linear relationship between the cos θ_a and X_{eda} was still obeyed.

d. Characterization of Surface EDA Reactivity with 13F. As shown above, EDA films become completely photolyzed by 193-nm radiation at energies of >10 J/cm^2. Unlike EDA, 13F

(23) Bain, C. D.; Whitesides, G. M. *J. Am. Chem. Soc.* **1988**, *110*, 3665–3666.
(24) Bain, C. D.; Whitesides, G. M. *J. Am. Chem. Soc.* **1988**, *110*, 6560–6561.
(25) Chattoraj, D. K.; Birdi, K. S. *Adsorption and the Gibbs Surface Excess*; Plenum Press: New York, 1984.
(26) Cassie, A. B. *Discuss. Faraday Soc.* **1948**, *3*, 11–16.
(27) Israelachvili, J. N.; Gee, M. L. *Langmuir* **1989**, *5*, 288.

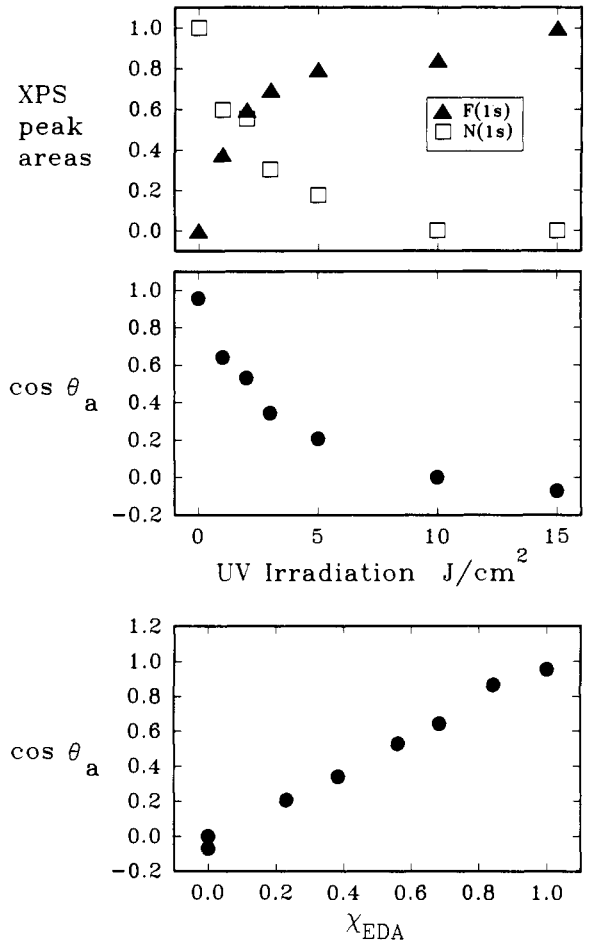

Figure 2. (Top, middle): Surface characteristics plotted against increasing levels of 193-nm deep UV radiation (abscissa) followed by exposure to a reactive mixture of 13F in toluene. Top: XPS peak areas. N(1s) (squares) and F(1s) (triangles) peaks are normalized to those obtained for pure EDA and 13F films, respectively. The data points at 0 and 15 J/cm^2 are those obtained for pure EDA (unirradiated and not exposed to 13F) and completely photolyzed EDA, respectively. Middle: Decreasing cos (θ_a) values reflected the changes in composition of the monolayers. Bottom: Plot of cos (θ_a) versus the calculated EDA molar ratio, where X_{eda} = EDA/(EDA + 13F). The data points at cos (θ_a) = 0.0 and −0.07 correspond to SAMs prepared by using 10 and 15 J/cm^2, respectively. The error in the measurement is within the size of the symbols drawn in all plots.

films remain relatively unmodified, even at three times this dosage, as evidenced by only a 4–5° decrease in θ_a. Thus, exposure of the EDA monolayer, followed by 13F retreatment, is the only efficient sequence for patterning these particular molecules using two-step 193-nm deep UV lithography. However, this patterning sequence is complicated by at least partial reaction of available surface amine and/or silanol groups with 13F. We examined whether this could be due to the reaction of primary and secondary amine groups with the chlorosilane by using two model compounds, *tert*-butylamine and dibutylamine. Both types of amines showed strong evidence of rapid reaction with 13F in solutions of benzene. The HCl generated by the formation of the N–Si bond between the amine and the 13F would be expected to be scavenged by the excess amine, resulting in the formation of an insoluble quaternized ammonium salt, (as illustrated for the (n-Bu)$_2$NH reaction):

$$(n\text{-Bu})_2\text{NH} + \text{ClSiMe}_2(\text{CH}_2)_2\text{C}_6\text{F}_{13} \rightarrow (n\text{-Bu})_2\text{NSiMe}_2(\text{CH}_2)_2\text{C}_6\text{F}_{13} + \text{HCl}$$

$$\text{HCl} + (n\text{-Bu})_2\text{NH} \rightarrow (n\text{-Bu})_2\text{NH}^+\text{Cl}^- \text{ (insoluble)}$$

Consistent with this, the formation of an insoluble white precipitate was observed within 5 min for both amines. The NMR spectra of the soluble material (not shown) were consistent with the formation of (t-Bu)NH-SiMe$_2$(CH$_2$)$_2$C$_6$F$_{13}$, and (n-Bu)$_2$N-SiMe$_2$(CH$_2$)$_2$C$_6$F$_{13}$, resulting from the complete reaction of 13F with (t-Bu)NH$_2$ and (n-Bu)$_2$NH, respectively.

Table I. Solvent-Induced Changes in Wettability and Reactivity of Surface-Bound EDA[a]

solvent	$\theta_{a(H_2O)}$ (rinse) (deg)	$\theta_{a(H_2O)}$ (after 13F) (deg)	[13F]/[EDA]
H_2O	28		
Ph–CH_3	28	32	0.188
C_6H_{14}	28	45	0.068
CH_3OH	26		
$CHCl_3$	26	32	0.025
CH_3CN	20	69	0.151
$CHCl_3$:CH_3OH	20		

[a] EDA monolayers were prepared on fused silica slides and allowed to reach a steady-state $\theta_{a(H_2O)}$ value of 28°. Individual slides (each having $\theta_{a(H_2O)}$ = 28°) were sonicated for 2 min in different solvents, and baked for 5 min at 120 °C to remove the solvent. The advancing water contact angle, $\theta_{a(H_2O)}$ (rinse), was then immediately recorded. In all cases where a decrease was observed, the contact angle increased again to the steady-state value of 28°. Separate EDA-treated slides were treated with 2.0% 13F in each of the various solvents for 2 h. Each was subsequently rinsed four times in the appropriate solvent, baked for 5 min at 120 °C, and stored under helium for 4 h. The contact angle, $\theta_{a(H_2O)}$ (13F), was recorded after 4 h to allow comparison with the original contact angle. [13F]/[EDA] mol ratios on the same substrates were subsequently determined using XPS.

The fact that we observed only a limited reaction of 13F with the EDA monolayers suggested that some conformational states of the EDA on the surface might limit the accessibility of the amine groups.[20,21] As mentioned above, EDA exhibited a time-dependent increase in the advancing water contact angle. This was not initiated until after the bake step and could be delayed for at least several months if the EDA-treated substrates were stored in methanol prior to the removal of solvent. Ellipsometry performed on these substrates indicated that the increase of θ_a could not be attributed to the buildup of surface contamination, as no change in measured thickness was observed.

We explored the possibility of EDA conformational changes using several types of solvents and focussed on their ability to *regenerate* the low values of θ_a, which were observed immediately following the initial removal of methanol. Table I shows the effect on the θ_a of EDA films caused by brief (2 min) sonication in a variety of solvents followed by a 5-min bake at 120 °C. We found that the value of θ_a was largely unaffected by water and two nonpolar organic solvents, toluene and hexane. However, θ_a could be reduced partially by methanol and chloroform and almost completely by acetonitrile and 2:1 chloroform/methanol. In all cases where a decrease was observed, the contact angle again returned to 28° within 4–5 h. The process could be repeated at least three times with the same films, strongly suggesting a reversible, solvent-induced conformational change of the EDA molecules on the surface.

We examined the solvent dependency of the reaction of surface EDA with 13F using non-nucleophilic solvents of different polarity: hexane, toluene, chloroform, and acetonitrile. As shown in Table I, a correlation existed between the ability of the solvents to decrease the θ_a of EDA and their respective ability to allow the 13F reaction to increase the value of θ_a, with the most polar solvent, acetonitrile, causing the largest increase. However, the increased value of θ_a could not be correlated with the actual moment of 13F incorporated, as shown by the [13F]/[EDA] mole ratios in the last column of Table I. The most pronounced difference with respect to this was between substrates treated in toluene and acetonitrile, which had a large difference in θ_a despite a similar level of reaction with 13F. In contrast, EDA surfaces that were treated in toluene and chloroform had virtually identical values of θ_a despite a 6-fold decrease in the amount of 13F in the latter. Most interestingly, neither contact angle significantly exceeded the range of equilibrium values observed for pure EDA. Thus, the equilibrium surface energy would be nearly the same for EDA surfaces regardless of whether they were untreated or treated with

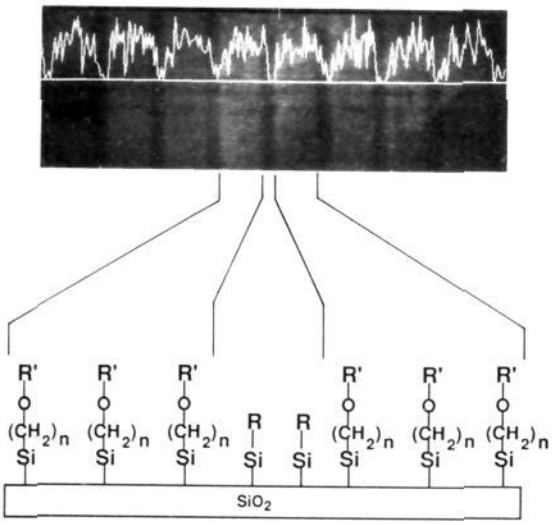

Figure 3. Scanning electron micrograph, Auger element line scan, and schematic representation of coplanar domains after patterning. The fluorine line scan is in registration with the irradiated areas and falls within the noise level in the nonirradiated areas. The light regions of the image, which are also present in nonfunctionalized surfaces that have been irradiated, may be due to an alteration of the hole density in the silicon. R and R′ are the same as in Scheme I. The scan represents raw data without spectral subtraction and is not inconsistent with the presence of a small amount of fluorine in the unirradiated areas.

13F in toluene or chloroform. Control experiments showed that 13F reacted equally well in hexane, toluene, chloroform, and acetonitrile to form monolayers with cleaned glass and native silicon oxide surfaces, as verified by contact angle and ellipsometric measurements. Therefore, the variations in the amount of incorporated 13F could not be attributed to differential effects of the solvents on the ability of 13F to react with nucleophilic species.

These results suggest that the reactivity of surface-bound EDA with the chlorosilane 13F is quite complex and that the choice of solvent may influence not only the degree but also the site(s) of reaction. However, two important points may be realized: (1) it appears that it is the free energy minimization of the EDA film itself that can, in several cases, dominate the equilibrium surface energy in the presence of low levels of 13F contamination and (2) through a judicious choice of the reaction solvent, the degree and/or effect of 13F contamination can be largely eliminated.

e. Characterization of EDA/13F Patterns with Auger Electron Spectroscopy. Side by side molecular domains were formed by exposure of EDA films on silicon to patterned UV at an energy of 15 J/cm^2, followed by retreatment with 13F. It has previously been demonstrated that scanning Auger electron spectroscopy (AES) is a useful technique for characterizing molecular monolayers at high spatial resolution.[15] We used AES to determine the lateral distribution of nitrogen and fluorine across alternating stripes of EDA and 13F. Figure 3 shows a fluorine element line scan across a series of 15 μm-wide EDA-rich lines separated by 45 μm-wide 13F lines. The scan is superimposed on a scanning electron micrograph of the corresponding pattern. We attribute the existence of the lighter regions of the image (which are also present on nonfunctionalized surfaces after irradiation) to a possible alteration of the hole density in the exposed silicon caused by irradiation. This fortuitous result, which allows image formation at low beam voltage and current, facilitates registration of the element line scans with the irradiated areas. As shown in Figure 3, the line scans confirmed what would be expected from the data presented in Figure 2: clearly delineated boundaries existed between the surface EDA-rich and 13F domains, as indicated by the sharp drop of the fluorine signal to within the noise level in the unirradiated areas.

f. Geometric Definition of Mammalian Cell Cultures. We have previously shown that EDA/13F patterns may be used to define the initial outgrowth patterns of a neuroblastoma cell line in vitro.[4] However, this effect was not demonstrated using dissociated cells from mammalian tissues, which are generally less adhesive and more dependent on the exact substrate composition for growth. In this study, we tested the ability of deep UV-defined SAM patterns to influence the adhesion and outgrowth of two types of explanted mammalian cells that form extended and complex architectures in vivo.

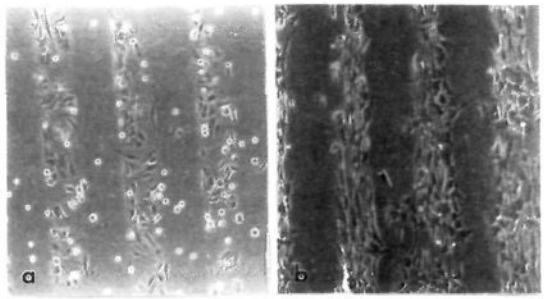

Figure 4. Porcine aortic endothelial cells on EDA/13F patterns. Cells in early passage were subcultured and seeded onto EDA/13F patterns. At 4 h after seeding (panel a), the cells exhibited differential attachment and spreading on 100 μm-wide EDA lines. The growth medium and unattached cells were subsequently removed by rinsing with fresh media, and the incubation continued. At 90 h after seeding (panel b), the cell remained oriented along, and largely restricted to, the EDA lines. The arrowhead denotes a small percentage of cells that have crossed into the 13F region.

Endothelial cells form the walls of arteries, veins, and capillaries. In vivo, the cells adhere to an extracellular matrix that includes mixtures of complex proteins and carbohydrates. In vitro, the cells are typically cultured on collagen- and/or fibronectin-coated substrates and are known to have the capacity to self-assemble from monolayers into neovascular chordes.[16] It would be of great value to have the ability to arbitrarily determine the geometry of these structures.

Preliminary results (not shown) indicated that EDA provided a suitable substrate for the normal morphological development of these cells, while 13F resisted adhesion. This should be expected, since the EDA provides a hydrophilic, positively-charged surface that should interact well with the external surfaces of cells, which generally have a net negative charge.[28] Cells were cultured on EDA/13F patterns prepared on glass microscope slides. The endothelial cells attached to the EDA-rich regions within 4 h (Figure 4a) and spread to adopt the same morphology as on pure EDA. On the 13F regions, the cells were more rounded and optically refractile after 4 h, indicating incomplete attachment. By 90 h after plating (Figure 4b), several rounds of cell division resulted in an increase in cell density and formation of cellular multilayers in the direction normal to the substrate surface. However, the spread of the cells was still substantially defined by the EDA/13F junction. We suggest that endothelial cell patterns at this and subsequent time points may be quite useful as starting points for growth factor-induced formation of neovascular chords.[29]

One of the most compelling reasons for defining two-dimensional growth patterns of cells in vitro is the direction of neural cell outgrowth and formation of synaptic interconnections. Dissociated neurons from the rodent hippocampus are ideal candidates for this purpose, since they demonstrate synapse formation and modification reflective of neurons in vivo.[30] However, their geometrical patterns of axon and dendrite growth on homogeneous substrates are random and highly overlapping, complicating the study of simplified synaptic circuits.

We conducted preliminary experiments which showed that both EDA, and EDA exposed to 13F in toluene, were equally effective

(28) Alberts, B.; Bray, D.; Lewis, J.; Raff, M.; Roberts, K.; Watson, J. D. *The Molecular Biology of the Cell*; Garland Publishing, Inc.: New York, 1989.

(29) Ingber, D. E.; Folkman, J. *J. Cell Biol.* **1989**, *109*, 317–330.

(30) (a) Bekkers, J. M.; Richerson, G. B.; Stevens, C. F. *Proc. Natl. Acad. Sci. U.S.A.* **1990**, *87*, 5359–5362. (b) Bekkers, J. M.; Stevens, C. F. *Nature* **1990**, *346*, 724–729.

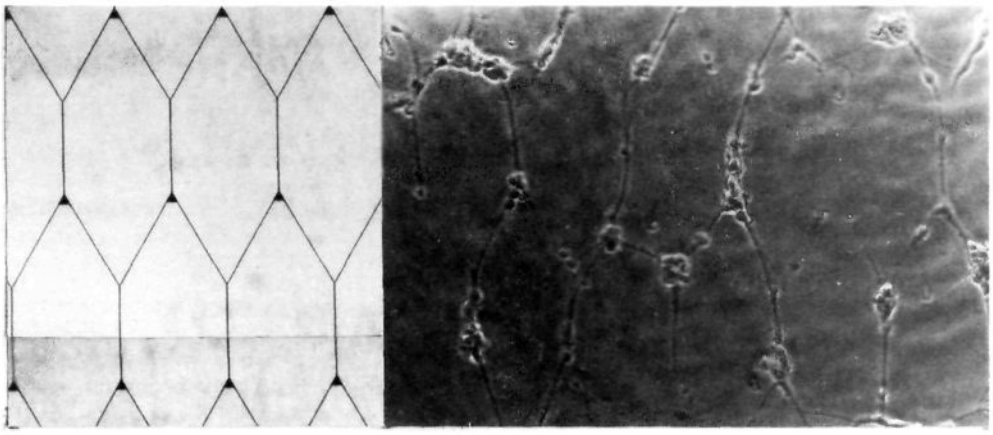

Figure 5. Photolithographic definition of neural cell morphologies. (left) Metalized mask design for preferential cell body adhesion and directional definition of subsequent neurite outgrowth. The lateral separation between triangular cell adhesion points is 200 μm. (right) Hippocampal cells extending processes on EDA pathways at 48 h after plating.

in promoting adhesion and neurite outgrowth of dissociated embryonic day 18 (E18) hippocampal neurons. A special mask (Figure 5, left panel) was designed to allow lithographic definition of triangle-shaped EDA regions (triangle sides range from 5–20 μm) which would be large enough to allow adhesion when the cells are initially plated. Narrow lines (widths range from 1.0–3.0 μm) in the mask allowed definition of EDA channels that were not wide enough to allow cell body adhesion during plating but provided pathways for the exploratory growth cones of the developing neurons. Dissociated cells from E18 rats were plated on inverted substrates having EDA/13F patterns defined by the mask. Figure 5 (right panel) shows the resultant pattern of hippocampal cells that had developed at 48 h after plating. In general, cell adhesion occurred only at the triangular sites (where multiple cells often accumulated) and in regions where three EDA lines intersected. Neurite processes were almost exclusively directed along the EDA pathways. Cells did not develop neurites on patterns having EDA triangles without interconnection pathways (not shown). Work is currently underway to determine the physiological properties of synaptic connections formed between neurons on these types of patterns.

Discussion

We have described conditions for the formation of self-assembled monolayers on silica surfaces from two materials: EDA, an aminoalkyltrimethoxysilane, and 13F, a perfluorinated monochlorosilane. Both formed films having measured thickness of about half of those predicted for the molecules fully extended normal to the substrate plane. Our thickness measurements for both EDA and 13F for EDA cannot be attributed to insufficient reaction times and are consistent with the formation of reaction-site limited monolayers. It has long been inferred that the amine groups of EDA molecules can participate in hydrogen bonding with side-chain silanols, causing a reduction in their reactivity.[20] Our thickness measurements were not inconsistent with this, but it should be emphasized that the measurement represents an *average* thickness over a relatively large area (10^4 μm^2).

Salaneck[31] et al. used angle-dependent XPS to estimate the thickness and molecular orientation of the films prepared from the dichloro version of 13F, (tridecafluoro-1,1,2,2-tetrahydrooctyl)-1-methyldichlorosilane on silicon. They reported an estimated thickness of 6 Å, which approached that predicted for a closely-packed monolayer of molecules having a tilt angle of half the tetrahedral angle (55°). Our thickness measurements for 13F were consistent with this observation. Our measured value of θ_a for 13F was approximately 18° lower than those reported for SAMs prepared from *n*-octadecyltrichlorosilane[32] and 24° lower than SAMs prepared from a comparable length perfluorinated alkyl thiol.[10] These results suggest that the lower water contact of 13F films may be related to both (a) the lower molecular packing density of monochlorodimethylsilane-derived SAMs[33] compared to those prepared from trichlorosilanes and alkanethiols and (b) the resulting reduction in the ability to shield the polar substrate from water.

The 193-nm radiation dosages in the range of 1–15 J/cm^2 at 193 nm cause partial to complete photolytic removal of the amine functional groups from EDA, leaving only silanol or short chain (≤3 carbon) alkyl derivatives. The formation of free-radicals during photolysis[34] could conceivably generate oxidized surface residues by reaction with atmospheric water.[4] These nucleophilic species react with the chlorosilane 13F in a subsequent step. Continuously variable free energy surfaces may be fabricated with this technique, making deep UV defined SAMs attractive model systems. We have reported for the first time the controllable formation of mixed monolayers consisting of varying mole fractions of an aminoalkylsilane and a perfluoroalkylsilane. The surface free energy of these monolayers was related to the EDA mole fraction in an almost linear fashion. This may be a reflection of (a) the disorder of the films (resulting in an increased distance between polar groups) relative to well-ordered alkanethiol films and (b) the possibility that hydrogen bonding may be stronger between amine and water molecules than between two amine groups. However, the lack of close-packing and order in these monolayers does not inhibit their ability to be used in conjunction with UV irradiation to "tune" the surface free energy.

We have provided indirect evidence that the EDA molecules are capable of undergoing reversible solvent-induced conformational changes. This effect was strikingly reminiscent of the behavior reported recently by Evans et al.[35] for –OH terminus alkanethiols on gold. They demonstrated that these molecules probably undergo free energy-minimizing conformational changes in the course of hours following the removal of polar solvent. We show here that the degree and possibly the site(s) of the reaction of 13F with EDA-treated surfaces are also solvent-dependent. The possible role of these solvents in changing the protonation state of the EDA must also be considered in future experiments. In all cases, the extent of the reaction of EDA films with 13F was much less than that expected in solution or between surface-bound EDA (on metal oxides) with acyl chlorides.[20] We have used this knowledge to largely eliminate the effects of 13F contamination into the EDA monolayers, allowing the formation of geometric coplanar assemblies having dramatically different surface energies.

(31) Salaneck, E. W.; Uvdal, K.; Elwing, H.; Askendal, A.; Welin-Kindström, S.; Lündstrom, I.; Salaneck, W. R. *J. Colloid Interface Sci.* **1990**, *136*, 440–446.

(32) Maoz, R.; Sagiv, J. *J. Colloid Interface Sci.* **1984**, *100*, 465–496.

(33) Riedo, F.; Czencz, M.; Liardon, O.; Kovats, E. *Helv. Chim. Acta* **1978**, *61*, 1912–1941.

(34) Coyle, J. D. *Introduction to Organic Photochemistry*; John Wiley & Sons: New York, 1986.

(35) Evans, S. D.; Sharma, R.; Ulman, A. *Langmuir* **1991**, *7*, 156–161.

It is clear that much work needs to be done to address the relationship between solvent-induced conformation and reactivity of SAM functionalities.

The free energy of cell adhesion on solid surfaces is determined by the interfacial tensions between the cell, substrate, and liquid media.[36] EDA is suitable for the patterned adhesion of at least five types of cells (this report and refs 2 and 4), suggesting that it is the overall electrostatic and thermodynamic properties of the EDA and 13F surfaces that determine the adhesion, rather than a type of specific recognition between molecules on the substrate and cell surfaces. In this case, EDA (and unirradiated EDA exposed to 13F) provided suitable growth substrates for two types of explanted mammalian cells for which the standard growth substrates are loosely-packed polymers (polylysine, collagen). This suggests that the apparent disorder of EDA films might actually be *advantageous* for cell adhesion. The minor reaction of 13F with EDA-treated surfaces did not have a noticeable affect on cell adhesion. This is not surprising, since the equilibrium values of θ_a were nearly the same for pure EDA and for EDA treated with 13F in toluene or chloroform. It should be pointed out that proposed mechanisms of cell adhesion to SAMs must first account for the amount and nature of protein constituents of the cell culture media that bind to the substrate prior to the cells.[37,38]

Recent reports[39] indicate that silane-coupled cell adhesion peptide fragments can be used to affect the adhesion and growth of specific types of cells through molecular recognition. Future experiments may optimize the use of deep UV-defined patterns as templates for covalent attachment of these and other families of cell adhesion molecules[40] that may be used to further direct cell morphology and function.

Acknowledgment. This work was supported in part by the Office of Naval Research and the Office of Naval Technology (DAS), the Naval Medical Research Development Command (TBN; work unit No. MR04120.001-1002), and the MANTECH office of the Assistant Secretary of the Navy (J.M.C.). We acknowledge Steve McElvany for assistance with FTMS experiments and Tim Koloski (ONT Post-Doctoral Fellow) for NMR experiments. We thank Dr. Forrest Weight (National Institute of Alcohol Abuse and Alcoholism) for the generous use of animal care and cell culture facilities and Drs. Kenneth and Wendy Scholz (University of Chicago), and Gary Banker (University of Virginia) for advice and helpful conversations concerning neuron culture. We acknowledge the reviewers of this manuscript, whose careful attention to detail and constructive criticisms are greatly appreciated. The opinions and assertions contained herein are the private ones of the authors and are not to be construed as official or reflecting the views of the Navy Department or the naval service at large.

Registry No. EDA, 1760-24-3; 13F, 102488-47-1; silica, 7631-86-9.

(36) Dicosmo, F.; Facchini, P. J.; Neumann, A. W. *Colloids and Surfaces* **1989**, *42*, 255.
(37) Prime, K. L.; Whitesides, G. M. *Science* **1991**, *252*, 1164-1167.
(38) Lee, S. H.; Ruckenstein, E. *J. Colloid Interface Sci.* **1988**, *125*, 365-379.
(39) Massia, S. P.; Hubbell, J. A. *Anal. Biochem.* **1990**, *187*, 292-301.
(40) Albelda, S. M.; Buck, C. A. *FASEB J.* **1990**, *4*, 2868-2880.

Deuterium Isotope Effects in Constrained Tryptophan Derivatives: Implications for Tryptophan Photophysics

Lloyd P. McMahon, William J. Colucci,† Mark L. McLaughlin,* and Mary D. Barkley*

Contribution from the Department of Chemistry, Louisiana State University, Baton Rouge, Louisiana 70803-1804. *Received January 14, 1992*

Abstract: The deuterium isotope effect on the fluorescence quantum yield and lifetime of the constrained tryptophan derivative 3-carboxy-1,2,3,4-tetrahydro-2-carboline, W(1), was determined as a function of pH and temperature. The isotope effect between pH 3.5 and 11 is attributed to a temperature-dependent quenching process common to all indoles. At room temperature the quantum yield ratio in D_2O and H_2O is 1.05 for W(1) zwitterion and 1.7 for W(1) anion. The temperature dependence of the fluorescence lifetime was determined for the zwitterion and the anion in H_2O and D_2O. The frequency factors A and activation energies E^* in H_2O are $A = 6 \times 10^{16}$ s^{-1}, $E^* = 12.6$ kcal/mol for W(1) zwitterion and $A = 5 \times 10^{16}$ s^{-1}, $E^* = 11.8$ kcal/mol for W(1) anion, compared to $A = 8 \times 10^{16}$ s^{-1}, $E^* = 13.1$ kcal/mol for *N*-methylindole. The radiative rates, temperature-independent nonradiative rates, and activation energies E^* of W(1) zwitterion, W(1) anion, and *N*-methylindole are insensitive to solvent isotope. The frequency factors A of these compounds are 2- to 3-fold larger in H_2O than in D_2O. The large deuterium isotope effect in W(1) anion at room temperature compared to W(1) zwitterion results from two factors: a smaller temperature-independent nonradiative rate and a larger isotopically sensitive temperature-dependent rate. Several mechanisms for the intrinsic deuterium isotope effect are discussed. Two mechanisms are consistent with available data for indoles: "invisible" or incomplete proton transfer from water to indole and formation of a water–indole charge-transfer exciplex.

Tryptophan, W, has been much studied because of its importance as an intrinsic fluorescent probe of conformation and dynamics in proteins. The complex photophysics, however, make interpretation of fluorescence results difficult.[1] Multiexponential fluorescence decays appear to be the rule, rather than the exception, for tryptophan derivatives as well as for proteins containing a single tryptophan.[2] In some proteins the fluorescence decay of the single tryptophan approaches a continuous distribution of lifetimes.[3] One explanation for the lifetime heterogeneity invokes multiple ground-state conformers or microconformational states that do not interconvert on the fluorescence time scale. In the conformer model, the lifetime differences among conformers are attributed to differences in proximity of functional groups that

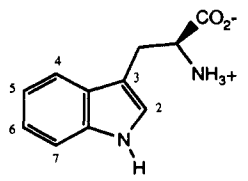

W

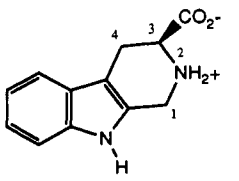

W(1)

† Present address: Ethyl Corp., Ethyl Technical Center, 8000 GSRI Ave., Baton Rouge, LA 70820.

(1) Creed, D. *Photochem. Photobiol.* **1984**, *39*, 537-562.
(2) Beechem, J. M.; Brand, L. *Annu. Rev. Biochem.* **1985**, *54*, 43-71.
(3) Alcala, J. R.; Gratton, E.; Prendergast, F. G. *Biophys. J.* **1987**, *51*, 925-936.

0002-7863/92/1514-8442$03.00/0